PHYSICAL REVIEW B **73**, 155205 (2006)

Electron-only diodes of poly(dialkoxy-*p*-phenylene vinylene) using hole-blocking bottom electrodes

M. M. Mandoc,* B. de Boer, and P. W. M. Blom

Materials Science Centre[Plus] and Dutch Polymer Institute, University of Groningen, Nijenborgh 4, 9747AG Groningen, The Netherlands*

(Received 17 November 2005; revised manuscript received 15 February 2006; published 10 April 2006)

Devices with two hole-blocking electrodes have been constructed to investigate the transport of electrons in a poly(dialkoxy-*p*-phenylene vinylene) (PPV) derivative. In order to test the compatibility with the solution processed PPV, a variety of hole-blocking bottom electrodes are applied and the absence of hole transport has been verified. The electron transport in PPV is strongly reduced as compared to the hole transport and exhibits a strong dependence on the applied voltage as well as sample thickness. These results are indicative for trap-limited electron transport with the energy of the trapping sites described by an exponential distribution.

DOI: 10.1103/PhysRevB.73.155205 PACS number(s): 72.20.Jv, 72.80.Le

I. INTRODUCTION

Since the discovery of electroluminescence in conjugated polymers,[1] the charge transport has been extensively studied in these materials. Because most of the conjugated polymers are *p*-type semiconductors, the focus has mainly been on the transport of holes.[2–6] However, it is evident that an understanding of the transport of electrons is essential for the optimization of double-carrier devices, such as polymer light-emitting diodes and polymer-based photovoltaic devices. Without an appropriate description of the electron transport, the electrical characteristics of these double-carrier devices cannot be described. Furthermore, an understanding of the electron transport can shed light on the question of why the transport in most conjugated polymers is dominated by holes. This can offer new insight into how one can chemically tailor the conjugated polymers in order to enhance their electron transport properties.

Experimentally, it has been shown that the electron current in poly(dialkoxy-*p*-phenylene vinylene) (PPV) derivatives is strongly reduced as compared to the hole current.[2,4] Furthermore, from time-of-flight measurements severe electron trapping in PPV has been demonstrated.[7] In one of the first studies on electron-only devices of conjugated polymers,[2] carried out on poly[2-methoxy-5-(3′, 7′-dimethyloctyloxy)-*p*-phenylene vinylene] (OC_1C_{10}-PPV), the strongly reduced electron current was explained by trap-limited conduction. The strong dependence of the electron current on applied voltage and sample thickness was in accordance with an exponential distribution of trapping sites in energy. Such an exponential trapping model had also been proposed by Burrows and Forrest[8,9] for the electron transport in aluminum hydroxyquinoline (Alq_3). In a more recent study, using thermally stimulated currents, the reduced electron currents were also attributed to traps,[10] which were related to the presence of oxygen. An alternative explanation for the reduced electron current in PPV-based electron-only devices is a space-charge limited (SCL) electron current, without traps, but assuming an intrinsically low electron mobility. This model was used to describe the electron current in poly[2-methoxy-5-(2′-ethylhexyloxy)-*p*-phenylene vinylene] (MEH-PPV), a material similar to OC_1C_{10}-PPV.[4] It was reported that the electron mobility in MEH-PPV is only one order of magnitude lower than the hole mobility and exhibits a stronger field dependence as compared to the hole current.

For characterization of the electron transport in PPVs, the devices have to be fabricated on hole-blocking contacts, which requires sufficiently low work function bottom electrodes. The first studies on OC_1C_{10}-PPV made use of Ca bottom electrodes.[2] However, low work function bottom electrodes, such as Ca or Ba, are highly reactive, and, therefore, less compatible with processing from solution. The electron transport in MEH-PPV was characterized using TiN as a bottom electrode.[4] However, whether this electrode was fully hole blocking was not verified. An interesting alternative would be silver (Ag), which is a nonreactive noble metal with a work function of only 4.3 eV. However, for a pure Ag bottom electrode, it has already been shown by van Woudenbergh *et al.*[11] that even a hole injection barrier of 0.95 eV is not sufficient to fully eliminate the contributions of holes. The presence of electrons leads to an enhancement of the hole injection in the device, due to the filling of electron traps at the polymer-Ag interface. These trapped electrons increase the field at the hole injecting contact, resulting in an enhancement of hole injection. In that case, the measured currents are not pure electron-only, but contain features of the injection-limited hole current.

So far, there is no consistent set of experimental data on the electron transport in PPVs available, and, therefore, no conclusive answer whether a low mobility or the presence of traps is responsible for the reduced electron current. In the present study, we test the suitability of a variety of metallic electrodes as hole-blocking bottom electrodes in our devices. For ytterbium (Yb) and aluminum (Al) bottom electrodes, the injection of holes is suppressed up to electric fields of 10^8 V/m. The strong voltage and thickness dependence of the electron current in these PPV-based diodes is in accordance with transport that is limited by traps, which are exponentially distributed in energy and located in the polymer bulk.

 ©2006 The American Physical Society

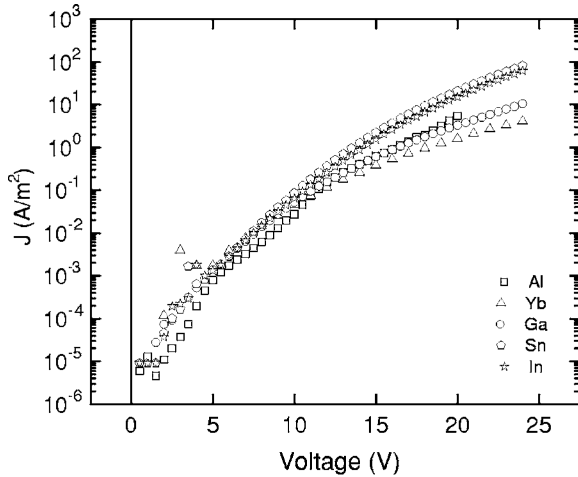

FIG. 1. *J-V* characteristics for different bottom electrodes: Al (square), Yb (triangle), Ga (circle), Sn (pentagon), and In (star). Thickness of the active layer is 200 nm for all devices.

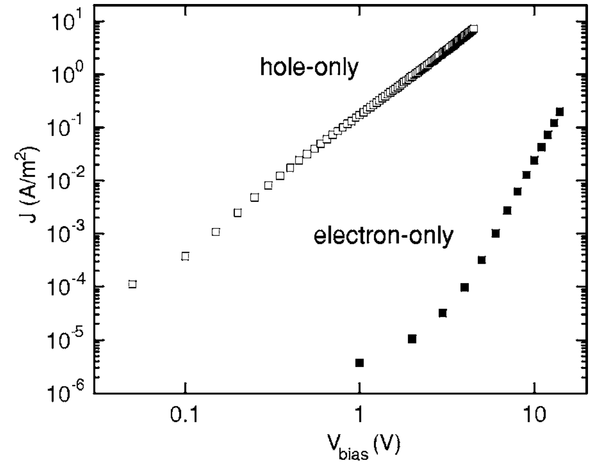

FIG. 2. *J-V* characteristics of a hole-only device (empty symbols) and of an electron-only device (filled symbols). The thicknesses of the active layers are 230 nm and 220 nm, respectively.

II. EXPERIMENT

Electron-only devices on a variety of metallic bottom electrodes were prepared. The bottom electrodes used were Yb, Ga, Sn, In, and Al. The electrodes were prepared by thermal evaporation at low pressure ($10^{-7}-10^{-6}$ mbar), with a thickness of 20 nm on top of indium tin oxide (ITO)-coated glass. Due to the limited thickness, all of these electrodes are semitransparent, allowing to observe light emission in the devices. Subsequently, poly[2-methoxy-5-(3′, 7′-dimethyloctyloxy)-*p*-phenylene vinylene] (OC_1C_{10}-PPV) was spin coated from toluene solution. Finally, barium (Ba) or ytterbium (Yb) top electrodes were vapor deposited and coated with a protective aluminum layer. All top electrode metals were evaporated at $\sim 10^{-7}$ mbar chamber pressure. Current density-voltage (J-V) measurements were performed in the dark and under a N_2 atmosphere, using a computer-controlled source meter unit Keithley 2400, and the eventual light output was measured by a photodiode connected to a Keithley 6514 electrometer. The J-V characteristics shown in our figures typically start from $J=10^{-5}$ A/m^2, which is determined by the sensitivity of the source-measure unit. With a typical device area of $\sim 10^{-5}$ m^2, this corresponds to a current of 100 pA. As an upper limit, we use the onset of the light-output, after which the measured currents are not intrinsically electron-only anymore.

III. RESULTS

A. Variation of metal bottom electrode

Figure 1 shows the current density J versus voltage V measured for OC_1C_{10}-PPV diodes made with Sn (work function 4.4 eV), Al (4.3 eV), Ga (4.2 eV), In (4.1 eV), and Yb (2.6 eV) (Ref. 12) bottom electrodes at room temperature. All of the devices have an Yb top electrode and the same thickness of the active layer. It is observed that at low voltages, all the *J-V* curves coincide, as expected for a truly electron dominated conduction. Only the *J-V* of the Al bottom electrode is slightly lower compared to the others. Since the metals used as bottom electrodes are reactive, it is likely that they form a protective oxide layer at the interface with the polymer. In case of Al, we observed with a Kelvin probe that the work function changed from 4.2 eV to 3.7 eV after the formation of the oxide layer. Such a change in work function modifies the built-in voltage and shifts the *J-V* along the voltage axis, which might explain the slightly different *J-V* for the Al electrode. The fact that the measured currents are nearly independent of the choice of the bottom electrode confirms the absence of chemical interactions between the bottom electrodes and the polymer. Such interactions might alter the current. Furthermore, for voltages larger than 10 V applied on devices with In and Sn, an enhancement of the current is observed, accompanied by the onset of light-output (not shown). This demonstrates that for these electrodes hole injection starts to occur, and the measured currents are not solely due to the electrons anymore.

In Fig. 2, the electron current is compared to the hole current in OC_1C_{10}-PPV. The current density versus applied voltage is plotted for an ITO/OC_1C_{10}-PPV/Au hole-only and Al/OC_1C_{10}-PPV/Yb electron-only device with a thickness of 230 nm and 220 nm, respectively. It is observed that the measured electron current is strongly reduced as compared to the hole current and exhibits a stronger field dependence, in agreement with earlier observations.[2] The fundamental question now arises as to whether the reduced electron current is a result of trapping[2] or of a low electron mobility.[4]

B. Thickness dependence of the electron current

The reduced electron current combined with its strong voltage dependence has been explained by electron traps that are exponentially distributed in energy.[2] In that case, the voltage dependence should be accompanied by a strong dependence of the current on sample thickness. In the exponential trap model, the current density scales with voltage and thickness according to:[13]

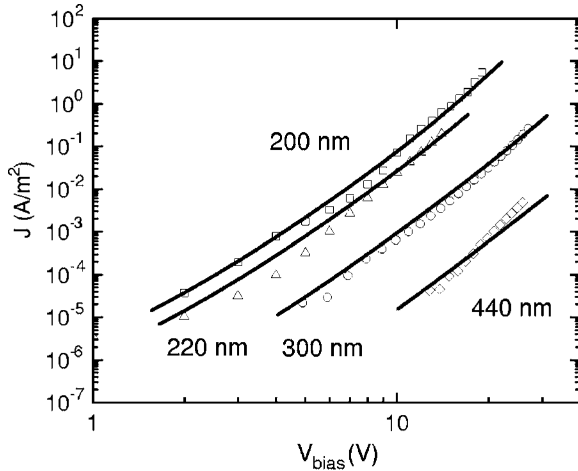

FIG. 3. Thickness dependent *J-V* characteristics for devices between 200 nm and 440 nm (symbols) and the simulation for the respective thicknesses (lines), using the exponential trap model, with $N_t=8.5\times10^{23}$ m^{-3} and $T_t=1500$ K, and a zero-field mobility of 5×10^{-11} m^2/V s.

$$J = N_c q \mu_n \left(\frac{\varepsilon_0 \varepsilon_r}{q N_t}\right)^r \left[\left(\frac{2r+1}{r+1}\right)^{r+1}\left(\frac{r}{r+1}\right)^r\right]\frac{V^{r+1}}{L^{2r+1}}, \qquad (1)$$

with q as the elementary charge, $\varepsilon_0\varepsilon_r$ as the dielectric constant, V as the applied voltage, L as the sample thickness, μ_n as the free electron mobility, N_c as the effective density of states, N_t as the amount of traps, and $r=T_t/T$, where T_t is the characteristic temperature of the exponential distribution. For $r>1$, the thickness scaling of this trap-limited current is stronger than the L^3 scaling that is expected for a SCL electron current with a low carrier mobility. In Fig. 3, the electron current densities versus applied bias for Al/OC_1C_{10}-PPV/Yb devices with thicknesses between 200 nm and 440 nm are shown. Although the measured electron currents exhibit a strong dependence on sample thickness, they do not show the expected power-law dependence on voltage, as predicted by Eq. (1). Such a power law would show up as a straight line in a log *J*-log *V* plot. The modeling of the measured *J-V* plots will be discussed in the following sections.

C. Trap-limited electron current versus low electron mobility

The voltage and thickness dependences of the experimental electron currents strongly support the concept of a trap-limited electron current,[2] as opposed to a low electron mobility.[4]

Another way to discriminate between these two mechanisms is to consider the current in a double carrier device, a light-emitting diode (LED). In Fig. 4, the experimental *J-V* characteristics of a hole-only diode and a LED (double carrier) of OC_1C_{10}-PPV are shown. It is observed that with increasing voltage the *J-V* characteristics diverge, reaching almost an order of magnitude difference at $V-V_{bi}=3$ V.

Subsequently, we simulate the hole-only and double-carrier currents using a PLED device model[14,15] with equal values for the hole and electron mobility of 1.0×10^{-11} m^2/V s. Furthermore, a Langevin-type recombination is assumed.[16] Under the assumption of equal electron and hole mobilities, the difference between the calculated hole-only and double-carrier current (Fig. 5) is similar to the experimental data (Fig. 4). When we systematically lower the electron mobility by only one order of magnitude, the double-carrier current strongly decreases to the magnitude of the hole-only current. Further decreasing the electron mobility with another order of magnitude does not change the double-carrier current, as it is fixed to the hole-only current. In order to explain our measured electron currents with a low

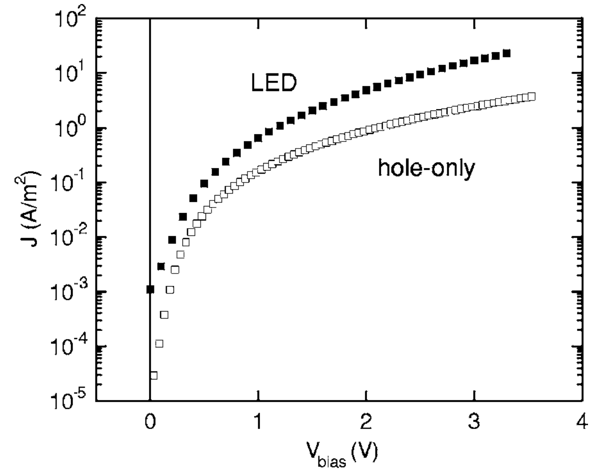

FIG. 4. Experimental *J-V* characteristics of an ITO/OC_1C_{10}-PPV/Au hole-only diode (empty symbols) and of a ITO/OC_1C_{10}-PPV/Ba/Al double carrier device (filled symbols). Both active layers are 230 nm thick.

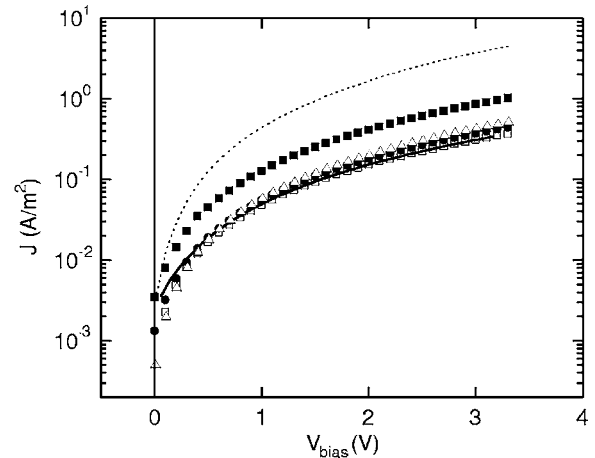

FIG. 5. Simulated *J-V* characteristics of hole-only device (empty squares) and of LED (filled squares) with equal electron and hole mobilities. The solid line and filled circles are the simulated LED currents, assuming an electron mobility of two orders of magnitude and one order of magnitude lower than the hole mobility, respectively. The dotted line and the empty triangles are the calculations with a Langevin recombination prefactor 20 times lower than that in the previous case, for equal mobility values, and for an electron mobility of two orders of magnitude lower than the hole mobility, respectively. The active layer thickness assumed in the simulation is 230 nm.

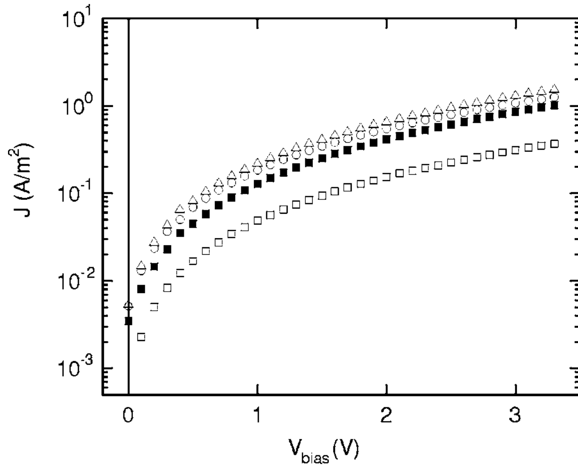

FIG. 6. Simulated *J-V* characteristics of hole-only device (empty squares) and of LED (filled squares) with equal electron and hole mobilities. The empty circles and triangles are the simulated LED currents, assuming a trapped electron current with $N_t=5.0\times10^{23}$ m^{-3} and 2.0×10^{24} m^{-3}, respectively, and $T_t=1300$ K. The active layer thickness assumed in the simulation is 230 nm.

electron mobility, a three orders of magnitude difference between electron and hole mobility would be required. Figure 5 clearly demonstrates that for such low electron mobilities, no difference between a double-carrier and hole-only current would be observed, in contrast to the experimental results of Fig. 4. The magnitude of the double-carrier current also depends on the strength of the bimolecular recombination. However, if the recombination is taken much weaker as compared to the Langevin type, it does not significantly affect the modeling results. In the case of a large mobility difference, for example $\mu_h \gg \mu_e$, the electrons are strongly confined to a region close to the cathode. As a result, a large mobility difference spatially separates the electrons and holes. The consequence of this is that the LED current becomes relatively insensitive to the Langevin prefactor, while for equal mobilities, the effect of a reduced Langevin prefactor is much stronger. The modeling results, assuming a Langevin recombination prefactor 20 times lower than that in the previous case, are shown also in Fig. 5. It can be seen that while for equal mobilites the LED current significantly increases, the low electron mobility will produce the same effect as before, which is to lower the double-carrier current to the magnitude of the hole-only one.

Next, electron traps are introduced in the LED and we again start with a situation with equal electron and hole mobilities. In this model, an exponential distribution of trapping sites with density of traps N_t and trap temperature T_t, characteristic of the exponential distribution, is chosen. The density of traps (N_t) is gradually increased from 5×10^{23} m^{-3} to 2×10^{24} m^{-3}. From Fig. 6, we can observe that the magnitude of the current for the double-carrier device remains the same, and the number of traps assumed in the material has only a weak influence on the current.

Our calculations in Fig. 6 show that the double-carrier current slightly increases when the amount of electron traps is increased, which seems counterintuitive. However, it should be noted (Fig. 2) that the hole current is orders of magnitude higher than the electron current, and therefore will dominate the current in the LED. The fact that the current of a LED is higher than the current of a hole-only device originates from the fact that, since electrons neutralize holes, an LED contains more of the mobile holes than a hole-only device. The small increase in the current density with the number of electron traps is due to the fact that at a higher trap density more electrons are trapped, which will increase the density of holes that can enter the device. Even though the electron current is lower, the hole current will become higher, leading to the small increase in the total current of the LED. At very low voltages, the amount of electrons is low and the amount of holes in the LED will not be that much different from a hole-only device, leading to an almost identical current.

The difference in the order of magnitude of experimental (Fig. 4) and calculated currents (Figs. 5 and 6) comes from the assumption of a constant mobility in the simulations. In recent studies, we have demonstrated that at room temperature the hole mobility in a PPV SCL current increases mainly due to an increase of the density.[17,18] We also observed by studying various PPV derivatives that this density dependence changes when the mobility is changed. This means that when we would like to systematically vary the mobility of one of the carriers, as in Figs. 5 and 6, the density dependence also has to be adapted for every mobility used. Since there is no explicit relation known between density dependence and magnitude of the mobility, the calculations would strongly depend on the choice of the density dependence. To avoid these complications, we used a constant mobility, which does not change the physics: By lowering the electron mobility, the electron density in the LED will be more closely confined to the cathode and the current will more and more resemble that of a hole-only device.

These modeling calculations demonstrate that in order to explain the enhanced double carrier currents of Fig. 4 "fast" free electrons must be present in the LED, with mobilities of the same order of magnitude as the hole mobility. The existence of fast free electrons has recently been demonstrated by Chua *et al.*,[19] where electron currents in OC_1C_{10}-PPV with magnitudes comparable to hole currents have been observed in field-effect transistors. This was achieved by using a gate dielectric free of electron traps. It should be noted that the density of electron traps required to explain our reduced electron currents is typically $\sim10^{18}$ cm^{-3}. For a transistor, this density is already reached with $\sim$2 V on the gate.[17] As a result, for larger gate voltages, these traps are filled and free electron currents are expected, as observed by Chua *et al.*[19] Concluding, the assumption of a low electron mobility contradicts the enhanced currents observed in double-carrier LEDs. The trap model, on the other hand, can simultaneously explain the enhanced double-carrier currents and reduced electron-only currents.

IV. DISCUSSION

A. The mobility of free electrons

In order to apply a trap-limited model as given by Eq. (1), the mobility of free electrons μ_n needs to be taken into ac-

count. In a recent study by Chua *et al.*,[19] it was shown that in field-effect transistors the free electrons are as mobile as holes for the PPV derivative studied here. Therefore, we assume the same mobility expression for the free electrons as the one recently derived from trap free hole transport. It has been shown that the mobility of free holes in conjugated polymers is strongly temperature dependent,[2–6] originating from hopping in a broadened density of states.[20] For SCL diodes based on OC_1C_{10}-PPV, it was also observed that the current strongly increases with increasing voltage, which was attributed to the field dependence of the hole mobility.[3,5] However, Tanase *et al.* demonstrated that at room temperature the hole mobility in PPV derivatives is not dependent on the field,[3,4] but on the carrier density.[16,17] Theoretical calculations of Arkhipov *et al.* have already predicted this kind of dependence,[21] on which further work has been carried since[22,23]. At room temperature, the hole mobility is described by the following expression:[17,24]

$$\mu_h(p,T) = \mu_h(0,T) + \frac{\sigma_0}{e}\left[\frac{\left(\frac{T_0}{T}\right)^4 \sin\left(\pi\frac{T}{T_0}\right)}{(2\alpha)^3 B_c}\right]^{T_0/T} p^{T_0/T-1}, \quad (2)$$

where σ_0 is a conductivity prefactor, α^{-1} is the effective overlap parameter between localized states, B_c is the critical number for the onset of percolation, and T_0 is the measure of the width of the exponential density of states.[16] All of the parameters from the second term of Eq. (2), containing the charge carrier density dependence, are derived from transistors measurements.[16,24] Theoretical model calculations further demonstrated that at low temperatures the electric field contribution also has to be taken into account.[25] Furthermore, these model calculations revealed that the field dependence of the mobility can be approximately modeled with a charge carrier density independent prefactor $f(T,E)$, meaning that $\mu(p,T,E) \approx \mu(p,T)f(T,E)$. Therefore, we approximate the mobility as

$$\mu(p,T,E) = \mu(p,T)\exp(\gamma\sqrt{E}), \quad (3)$$

with $\mu(p,T)$ given by Eq. (2). In Eq. (3), the electric field coefficient γ is zero at room temperature because the mobility is dominated by the charge carrier density dependence. With decreasing temperature, it approaches the earlier reported values[3,5] that were obtained under the assumption that the mobility was solely governed by its field and temperature dependence (Fig. 7).[2–6]

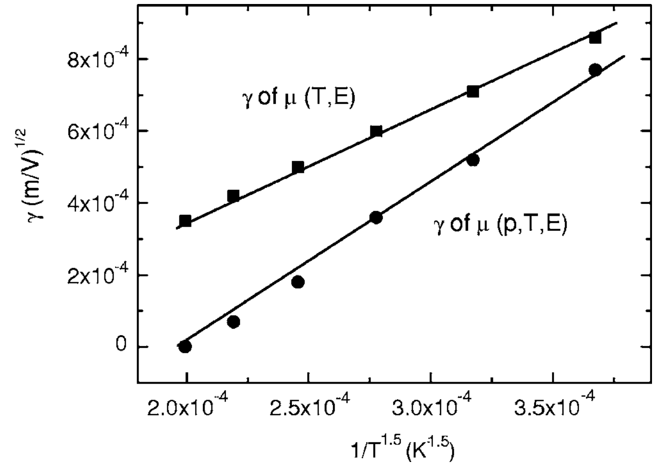

FIG. 7. The values of the electric field coefficient γ for OC_1C_{10}-PPV. The squares represent the earlier reported values assuming a field and temperature dependent mobility. The circles take into account the charge carrier density dependence. The lines are a guide for the eyes.

B. Initial trap filling due to carrier diffusion

In the derivation of the trap-limited current, given by Eq. (1), the effect of carrier diffusion has been ignored, only carrier drift has been taken into account.[13] However, diffusion can play an important role when an ohmic contact is formed between a metal and a semiconductor containing traps. In order to equilibrate the Fermi level, electrons will diffuse into the semiconductor, thereby filling traps that are located close to the electrode (inset Fig. 8). When a voltage is applied and electrons are injected into the semiconductor, these filled traps will not participate in the electron trapping process. As a result, the trap-limited current will be higher than expected from the models where only the drift current is taken into account and all of the traps are assumed to be empty. It is clear that the effect of the diffusion-induced trap-filling will be larger for the thinner devices. In Fig. 8, the effect of trap filling due to carrier diffusion is demonstrated for a device with two ohmic contacts, as well as a device with one ohmic and one neutral contact (meaning that there is no charge transfer, as is the case for a high injection barrier). For electron-only devices discussed here, a neutral/ohmic contact device model has been assumed. As can be derived from Fig. 8 even at 20 nm away from the Ohmic contact, still 5.9% of the traps are filled.

The effect of diffusion on the calculated *J-V* characteristics is demonstrated in Fig. 9 for a 220 nm thick device. For

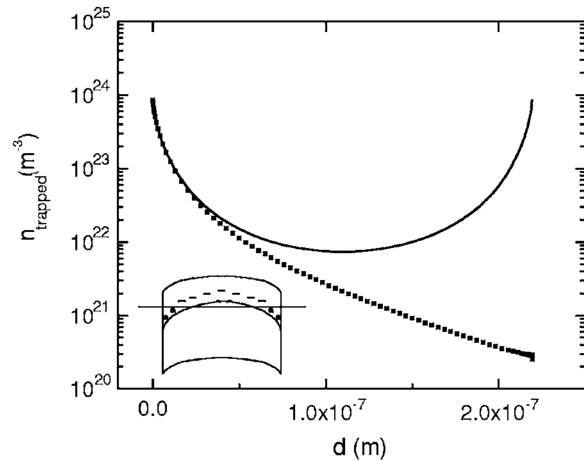

FIG. 8. Density of trapped carriers of an ohmic/neutral contact device (symbols), and of an ohmic/ohmic contact device (line) versus the distance from the ohmic contact (d). The simulations are made for 0 V and assuming an active layer thickness of 220 nm. The inset shows a schematic band diagram of a device with two ohmic contacts.

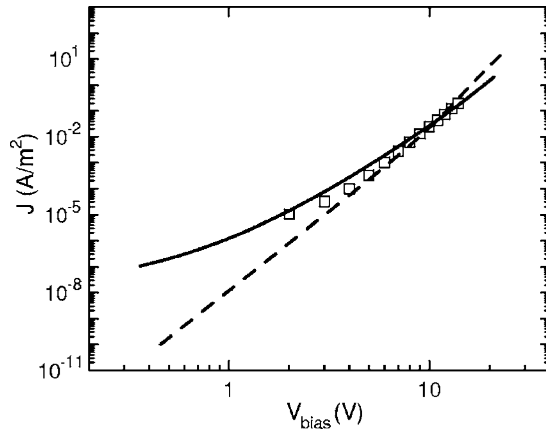

FIG. 9. Electron current for a 220 nm thick device (squares), and the simulations with drift and diffusion (solid line) and only drift (dash line), with N_t=8.5×10^{23} m^{-3} and 7.0×10^{23} m^{-3}, respectively.

comparison, the simulations including both drift and diffusion, and only drift are plotted, together with the experimental data of an Al/OC_1C_{10}-PPV/Yb device (symbols). In the drift and diffusion model, an Ohmic and neutral contact have been assumed, in accordance with the work functions of Yb and Al, respectively. A zero-field free electron mobility of 5×10^{-11} m^2/V s was used in the simulations, with T_t =1500 K. It is demonstrated that the steeper increase of the drift-only simulation approximates the experimental data at high voltages, where most of the traps are filled. The gradual increase of the experimental electron-only current is represented by the simulations when diffusion is taken into account. More details about the numerical schemes used in the drift-diffusion simulation can be found in Ref. 26.

In Fig. 3, the electron current for Al/OC_1C_{10}-PPV/Yb devices with thicknesses between 200 nm and 440 nm are shown. The predictions of the exponential trap model including diffusion are also included as solid lines. Using the trap parameters N_t=8.5×10^{23} m^{-3} and T_t=1500 K, and a zero-field mobility of 5×10^{-11} m^2/V s, we observe that both voltage and thickness dependence are in good agreement with the experimental data. The trap parameters used are nearly identical to the ones previously reported for Ca/OC_1C_{10}-PPV/Ca devices.[2] Thus, it can be concluded that the exponential trap model gives a good description of the electron current at room temperature. Further studies of the temperature dependence of the electron current need to be done to further elucidate the details of the charge transport mechanism and the origin of the electron traps.

V. CONCLUSIONS

We have measured the electron current in OC_1C_{10}-PPV using a variety of electrodes that block the hole injection. The strong voltage and thickness dependence of the experimental electron currents are consistently explained by trapping of electrons in an exponential distribution of traps. Unlike the concept of an intrinsically low electron mobility, the presence of electron traps in the bulk of the polymer is also consistent with the enhanced currents observed in OC_1C_{10}-PPV-based LEDs.

ACKNOWLEDGMENTS

We acknowledge Cristina Tanase, Jan-Anton Koster, and André Hof for their assistance, and Minte Mulder for technical support. This work is part of the research program of Dutch Polymer Institute (Project No. 324).

*Electronic address: m.m.mandoc@rug.nl

[1] J. H. Burroughes, D. D. C. Bradley, A. R. Brown, R. N. Marks, K. Mackay, R. H. Friend, P. L. Burns, and A. B. Holmes, Nature (London) **347**, 539 (1990).
[2] P. W. M. Blom, M. J. M. de Jong, and J. J. M. Vleggaar, Appl. Phys. Lett. **68**, 3308 (1996).
[3] P. W. M. Blom, M. J. M. de Jong, and M. G. van Munster, Phys. Rev. B **55**, R656 (1997).
[4] L. Bozano, S. A. Carter, J. C. Scott, G. G. Malliaras, and P. J. Brock, Appl. Phys. Lett. **74**, 1132 (1999).
[5] P. W. M. Blom and M. C. J. M. Vissenberg, Mater. Sci. Eng., R. **27**, 53 (2000).
[6] H. C. F. Martens, P. W. M. Blom, and H. F. M. Schoo, Phys. Rev. B **61**, 7489 (2000).
[7] H. Antoniadis, M. A. Abkowitz, and B. R. Hsieh, Appl. Phys. Lett. **65**, 2030 (1994).
[8] P. E. Burrows and S. R. Forrest, Appl. Phys. Lett. **64**, 2285 (1994).
[9] Z. Shen, P. E. Burrows, V. Bulovic, D. M. McCarty, M. E. Thompson, and S. R. Forrest, Jpn. J. Appl. Phys., Part 2 **35**, L401 (1996).
[10] V. Kazukauskas, H. Tzeng, and S. A. Chen, Appl. Phys. Lett. **80**, 2017 (2002).
[11] T. van Woudenbergh, P. W. M. Blom, and J. N. Huiberts, Appl. Phys. Lett. **82**, 985 (2003).
[12] S. M. Sze, *Physics of Semiconductor Devices*, 2nd ed. (Wiley, New York, 1981).
[13] K. C. Kao and W. Hwang, *Electrical transport in solids* (Pergamon Press, Oxford, 1981).
[14] P. W. M. Blom, M. J. M. deJong, and S. Breedijk, Appl. Phys. Lett. **71**, 930 (1997).
[15] B. K. Crone, P. S. Davids, I. H. Campbell, and D. L. Smith, J. Appl. Phys. **84**, 833 (1998).
[16] U. Albrecht and H. Bassler, Phys. Status Solidi B **191**, 455 (1995).
[17] C. Tanase, E. J. Meijer, P. W. M. Blom, and D. M. deLeeuw, Phys. Rev. Lett. **91**, 216601 (2003).
[18] C. Tanase, P. W. M. Blom, and D. M. de Leeuw, Phys. Rev. B **70**, 193202 (2004).
[19] L. L. Chua, J. Zaumseil, J. F. Chang, E. C. W. Ou, P. K. H. Ho, H. Sirringhaus, and R. H. Friend, Nature (London) **434**, 194 (2005).

[20] H. Bassler, Phys. Status Solidi B **175**, 15 (1993).
[21] V. I. Arkhipov, P. Heremans, E. V. Emelianova, G. J. Adriaenssen, and H. Bassler, J. Phys.: Condens. Matter **14**, 9899 (2002).
[22] Y. Roichman, Y. Preezant, and N. Tessler, Phys. Status Solidi A **201**, 1246 (2004).
[23] R. Coehoorn, W. F. Pasveer, P. A. Bobbert, and M. A. J. Michels, Phys. Rev. B **72**, 155206 (2005).
[24] C. Tanase, P. W. M. Blom, D. M. de Leeuw, and E. J. Meijer, Phys. Status Solidi A **201**, 1236 (2004).
[25] W. F. Pasveer, J. Cottaar, C. Tanase, R. Coehoorn, P. A. Bobbert, P. W. M. Blom, D. M. de Leeuw, and M. A. J. Michels, Phys. Rev. Lett. **94**, 206601 (2005).
[26] L. J. A. Koster, E. C. P. Smits, V. D. Mihailetchi, and P. W. M. Blom, Phys. Rev. B **72**, 085205 (2005).